ACS APPLIED MATERIALS & INTERFACES

Research Article

www.acsami.org

Silicification of Genipin-Cross-Linked Polypeptide Hydrogels Toward Biohybrid Materials and Mesoporous Oxides

Jeng-Shiung Jan,* Pei-Shan Chen, Ping-Lun Hsieh, and Bo-Yu Chen

Department of Chemical Engineering, National Cheng Kung University, No. 1, University Rd., Tainan, Taiwan 70101, Republic of China

Supporting Information

ABSTRACT: A simple and versatile approach is proposed to use cross-linked polypeptide hydrogels as templates for silica mineralization, allowing the synthesis of polypeptide−silica hybrid hydrogels and mesoporous silica (meso-SiO_2) by subsequent calcination. The experimental data revealed that the cross-linked polypeptide hydrogels comprised of interconnected, membranous network served as templates for the high-fidelity transcription of silica replicas spanning from nanoscale to microscale, resulting in hybrid network comprised of interpenetrated polypeptide nanodomains and silica. The mechanical properties of these as-prepared polypeptide−silica hybrid hydrogels were found to vary with polypeptide chain length and composition. The synergy between cross-link, hydrophobic interaction, and silica deposition can lead to the enhancement of their mechanical properties. The polypeptide−silica hybrid hydrogel with polypeptide and silica content as low as 1.1 wt % can achieve 114 kN/m^2 of compressive strength. By removing the polypeptide nanodomains, mesoporous silicas with average pore sizes ranged between 2 nm and 6 nm can be obtained, depending on polypeptide chain length and composition. The polypeptide−silica hybrid hydrogels demonstrated good cell compatibility and can support cell attachment/proliferation. With the versatility of polymer chemistry and feasibility of amine-catalyzed sol−gel chemistry, the present method is facile for the synthesis of green nanocomposites and biomaterials.

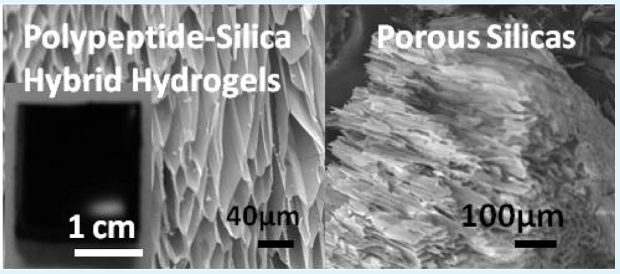

KEYWORDS: *hybrid hydrogels, nanocomposites, mineralization, polypeptide, cross-link, porous silica*

INTRODUCTION

Silica-condensing microorganisms such as diatoms and marine sponges have evolved mechanisms to create exquisite hierarchical structures over multiple length scales through precise control of nanoscale building blocks.[1−3] Proteins such as silaffins from diatoms and silicateins from marine sponges have been identified to play the key role on directing the uptake and organization of inorganic matter, leading to the formation of such intricate silica structures. Inspired by these silicification processes, there has been growing interest in developing and fabricating materials with new or unusual properties via template approaches.[4,5] A variety of self-assembled structures including micelles and nanofibers can serve as templates for the deposition of silica.[6−12] Secondary conformations of polypeptides such as α-helix and β-sheet can be replicated via silicification to produce microporous and mesoporous silicas.[9,13−16] In addition, the two-dimensional (2D) and three-dimensional (3D) silica architectures can be created by silica deposition into/onto the 2D or 3D patterns of scaffolds comprised of silica-condensing moieties with the aid of other techniques such as lithography and direct ink writing.[17−20] For example, Kaehr and co-workers reported the capability to create bioinspired silica microstructures with hierarchical feature over broad length scales using lithographically patterned protein hydrogels as templates. Peptidic moieties were commonly utilized to direct the deposition of silica onto the designated structures.

In addition to control silica nano- and microstructures, the ability to control silica deposition onto the scaffolds can result in hybrid materials with tunable properties, which might open up valuable opportunities for a variety of applications such as tissue engineering, green nanocomposites, and biosensing devices.[21−24] Previously, it has been demonstrated that the properties of hybrid materials can be tuned by controlling the constituent organic/inorganic weight ratio with the two phases interacting on a nanoscale.[6,25−29] Jones and co-workers reported the synthesis of gelatin−silica hybrid materials via covalent interactions between the organic and inorganic constituents, which enable the precise control of degradation and mechanical properties (compressive strength of 19−62 kN/m^2) by varying the constituent organic/inorganic weight ratio.[25] Pochan and co-workers reported the silica deposition onto the fibrillar nanostructures of self-assembled peptide hydrogels and the as-prepared peptide−silica hybrid hydrogels possessed tunable mechanical properties that can be achieved by controlling the thickness of the silica shell.[6] Amine-catalyzed

Received: September 17, 2012
Accepted: November 13, 2012
Published: November 13, 2012

sol−gel polycondensation resulted in the uniform silica coating on the peptide fibrils, which can potentially be a means to tune the constituent phases on a nanoscale. In addition to the constituent organic/inorganic weight ratio, controlling the chemistry of the organic phase can be the alternative approach to tune the properties of hybrid materials.

Herein, we report the synthesis and characterization of well-defined polypeptide−silica 3D networks via biomimetic silicification of cross-linked polypeptide hydrogels. The influence of polypeptide chemistry on the properties of the polypeptide−silica hybrid hydrogels and as-calcined silicas was investigated. Incorporation of hydrophobic block can facilitate self-assembly of the polypeptides and hence influence the properties of the as-prepared materials. Poly(L-lysine) (PLL) and block copolypeptides containing PLL were synthesized via living polymerization of *N*-carboxyanhydrides (NCAs) to yield well-defined chain length and composition.[30−32] Genipin was utilized to cross-link the lysine side chain to form hydrogels with interconnected, membranous networks and the lysine groups acted as directing agents for the condensation of silica precursor on the cross-linked polypeptide membranes. Polypeptide molecular weight, block ratio, and composition were varied to investigate the mechanical properties of the resulting silicified hydrogels. The silicified hydrogels were calcined and the porosities of silicas were characterized in order to investigate the interacting length scale of the polypeptide and silica phases. To evaluate the feasibility of using these materials for biomedical applications, a preliminary investigation on the cytotoxicity of the hydrogels and silicified hydrogels was carried out, as well as the cell attachment and proliferation on these hydrogels.

EXPERIMENTAL SECTION

Materials. L-alanine (>99%) and glycine (>99%) were used as received from Fluka and Merck, respectively. N_ε-Z-L-lysine (~99%, Z = carboxybenzyl), bis(1,5-cyclooctadiene) nickel(0) (98+%), and 2,2′-bipyridyl (99+%) were used as received from Sigma−Aldrich. Trifluoroacetic acid (99%) was supplied by Alfa Aesar. Triphosgene (98%), tetramethyl orthosilicate (99%), and hydrogen bromide (33 wt % in acetic acid) were used as-received from Fluka. Ethyl ether (ACS Reagent) and genipin (98%) were supplied by ECHO and Challenge Bioproducts Co. (CBC), respectively. THF (ACS Reagent, Merck) and hexane (ACS Reagent, EM Science) were dried using sodium metal and calcium hydride, respectively.

Polypeptide Synthesis. Homopolypeptides and block copolypeptides were synthesized using the nickel initiator 2,2′-bipyridyl-Ni(1,5-cyclooctadiene) (BpyNiCOD) by following the literature reported procedures.[30−32] These as-prepared N_ε-Z-L-lysine (Z-Lys), L-alanine (Ala), and glycine (Gly) *N*-carboxyanhydrides (NCAs) reacted with the nickel initiator in THF and the polymerization was carried out under inert conditions at room temperature. The NCAs were synthesized in dry THF using triphosgene as described by Daly and Poche.[33] The Z group on the side chain of poly(L-lysine) was deprotected by using hydrogen bromide. These as-prepared polypeptides were then dissolved in deionized (DI) water and dialyzed against DI water using a dialysis tubing (MWCO 6000−8000; Sigma, St. Louis, MO, USA). The water was exchanged 2−3 times per day over the next three days. Finally, these polypeptides were lyophilized using a freeze dryer to obtain white spongy materials. The notations for homopolypeptides and copolypeptides used throughout were Lys_m and Lys_mXa_n (Xa = Ala or Gly), where *m* and *n* are the number of amino acids in the respective block.

Preparation of Polypeptide−Silica Hybrid Hydrogels. The polyeptide hydrogels were prepared by the cross-linking reaction between genipin and the amine moieties in polypeptides. The freeze-dried polypeptides dissolved in DI water (5 wt %) were first prepared and the respective amount of genipin with a genipin/lysine molar ratio of 0.5 was added to the polypeptide solutions. The gelation was allowed to proceed at room temperature for at least two days. The hydrogels were dark blue in appearance. For silica deposition, these as-prepared hydrogels were immersed in freshly prepared 0.5 M orthosilicic acid solutions for 2−10 h to allow the deposition of silica in hydrogels. The polypeptide−silica hybrid hydrogels then were placed into DI water and washed by changing the water twice a day for at least two days. The as-prepared hybrid hydrogels were immersed in DI water before use. To remove organic compounds, these composite materials were lyophilized and calcined in air at 600 °C for 10 h (heating rate 10 °C/min).

Mechanical Properties. The compressive strengths of polypeptide hydrogels and polypeptide−silica hybrid hydrogels were determined using an MTS testing machine (AGS-X 500N, Shimadzu, Japan). Hydrogels with uniform rectangular shapes (n = 4) were prepared in Teflon mold and placed on the metal plate. The samples were then pressed at a speed of 0.5 mm/min to obtain the load−displacement curves.

In Vitro Cytotoxicity Tests. The fibroblast cells (3T3) were cultured onto a 48-well plate (1×10^4 cells/mL), using Dulbecco's modified eagle medium (DMEM, Gibco) with 10% BS (bovine serum, from Gibco) under a humidified atmosphere of 5% CO_2 at 37 °C. After culturing for 24 h, the medium was replaced with extract fluids obtained by placing the polypeptide hydrogels and polypeptide−silica hybrid hydrogels (0.1 g/mL of culture medium) in the cell culture medium at 37 °C for 24 and 48 h, respectively. The viability of adherent cells then was determined using the MTT assay.[34,35] By adding 3-(4,5-dimethylthiazol-2-yl)-2,5-diphenyltetrazolium bromide to the cells, the tetrazolium salt was converted to an insoluble purple formazan salt. After 4 h of incubation, the formazan salt was dissolved by a detergent solution. The resulting solution was measured at 570 nm, using an ELISA plate reader (Sunrise, Tecan). The number of viable cells can be quantified by measuring the absorbance intensity at 570 nm (n = 5). For the control experiment, the cells were grown in the culture medium under the same conditions. For cell adhesion test, fibroblast cells were seeded at 1×10^4 cells/mL onto the wells coated with the polypeptide or polypeptide−silica hydrogels. Cell cultured on the bare wells under the same condition acted as controls. After 24 h of culture, the adherent cells were observed using an inverted phase-contrast microscope.

Statistical Analysis. All data represent means ± standard deviations (SDs) for n independent determinations. Significance of results was determined with a Student's t-test on n independent measurements, where n is specified in the figure legend. Unless otherwise indicated, significance was taken as $p < 0.01$.

Instrumentation and Characterization. Gel permeation chromatography (GPC) measurements were performed before deprotection of the polypeptides, using a Viscotek system equipped with three detectors: a refractive index (RI) detector (VE3580, Viscotek), a right-angle light scattering detector, and a viscometer (Dual 270, Viscotek). Two ViscoGEL I-Series columns (Catalog Nos. I-MBHMW-3078 and I-MBLMW-3078, Viscotek) were used for efficient separation and eluted with 0.1 M LiBr in DMF at 55 °C. The eluent flow rate was 1 mL/min. ^{1}H NMR spectra were recorded at 300 MHz on a Mercury 300 Varian spectrometer using TFA-d_1 or D_2O as solvent. Field-emission scanning electron microscopy (FE-SEM) was performed using a JEOL JSM-6700F microscope operating at 1−10 kV. Samples were collected via lyophilization or calcination, and mounted on carbon tape for imaging. Transmission electron microscopy (TEM) images were taken with a Hitachi 700 system operated at an accelerating voltage of 100 kV. The samples were dispersed in methanol (100%, Aldrich) and dispensed on a carbon-coated copper grid. Fourier transform infrared (FTIR) spectra were recorded on a Thermo Nicolet Nexus 670 FTIR spectrometer. Circular dichroism (CD) spectra were measured over the wavelength range of 190−260 nm, using a 0.1 cm quartz cell on a JASCO Model J-815 spectrometer (JASCO, Inc., Japan). The hybrid hydrogels were ground into finely divided particles and suspended in aqueous solution for CD measurements. Nitrogen sorption measurements were

performed using a Micromeritics 2020 ASAP instrument at 77 K. Surface areas were calculated by the Brunauer–Emmett–Teller (BET) method. Pore volumes and pore size distributions were determined from nitrogen sorption isotherm data using the *t*-plot and the Barrett–Joyner–Halenda (BJH) method. The ratio of organic and inorganic content in the dried hybrid material was determined from the thermogravimetric analyses (Perkin–Elmer, TGA7 instrument). The range of the temperature was 25–800 °C, and the temperature ramping rate was 10 °C/min.

RESULTS AND DISCUSSION

The homopolypeptides and block copolypeptides were prepared by ring-opening polymerization. The molecular weight and block ratio of these polypeptides can be tuned by controlling the monomer and initiator concentrations, as well as the monomer/initiator ratio.[31] The list of homopolypeptides and block copolypeptides studied in this paper is summarized in Table 1. The molecular weights and polydispersities of these as-prepared polypeptides were determined by GPC (see Figure S1 in the Supporting Information). ^{1}H NMR measurements of these block copolypeptides in TFA-d_1 were performed to determine their block ratios. Poly(L-lysine)-block-poly(L-alanine) (PLL-b-PLAla) with different molecular weights and block ratios were used for the preparation of hydrogels. For comparison, the hydorgels prepared using poly(L-lysine) (PLL) with different molecular weights were also studied, as well as the hydrogels prepared using the block copolypeptides with different hydrophobic blocks such as polyglycine (PGly).

Table 1. Characterization of Homopolypeptides and Block Copolypeptides

sample code	polypeptide	block ratio[a]	M_n[b] [g/mol]	PDI[b]
a	Z-Lys_{120}		32 000	1.30
b	Z-Lys_{250}		65 600	1.20
c	Z-$Lys_{150}Ala_{25}$	6:1	41 400	1.22
d	Z-$Lys_{330}Ala_{55}$	6:1	95 500	1.17
e	Z-$Lys_{120}Ala_{15}$	8:1	34 700	1.09
f	Z-$Lys_{225}Ala_{28}$	8:1	61 000	1.28
g	Z-$Lys_{225}Gly_{38}$	6:1	61 500	1.56

[a]Determined by ^{1}H NMR in TFA-d_1. [b]PDI = M_w/M_n. The M_n and PDI values of the homopolypeptides and block copolypeptides were measured by GPC.

It was found that hydrogels can be prepared via either genipin or glutaraldehyde cross-linking with the amine moieties in polypeptides. In this study, polypeptides were cross-linked by genipin (see Scheme 1), which is a natural and nontoxic cross-linking agent and has been utilized to prepare polysaccharide hydrogels.[36−39] Recently, our group reported that vesicles assembled by alkyl-chain-grafted PLL can encapsulate biomolecules and subsequently the hydrophilic PLL can be cross-linked by genipin to form stable hydrogel particles.[40] The cross-link of polypeptides was carried out under mild conditions including aqueous solution, room temperature, and neutral pH. Previous studies have shown that poly(L-lysine)-b-poly(L-leucine) block copolypeptide can form hydrogels at low concentration.[41−43] These physically cross-linked hydrogels employed reversible physical interactions including ionic or hydrophobic interactions between polymer chains to form gel matrix. In this study, polypeptide hydrogels were prepared via chemical cross-link to form covalently bonded networks, which would have better physical stability in vivo and control of physical properties than physically cross-linked hydrogels. It was found that none of the polypeptides could form hydrogels, even at 9 wt %, if no genipin is added. The addition of genipin at 0.125–0.5 of genipin/lysine molar ratio to polypeptide solutions with concentration higher than 5 wt % can afford the formation of hydrogels. It is worth noting that the polypeptide solutions with lower concentration (<3 wt %) cannot form hydrogels, even after adding genipin. The solutions became

Scheme 1. (a) Schematic Illustration of the Formation of Polypeptide–Silica Hybrid Hydrogels and Porous Silicas and (b) Preparation of Polypeptide–Genipin Derivative

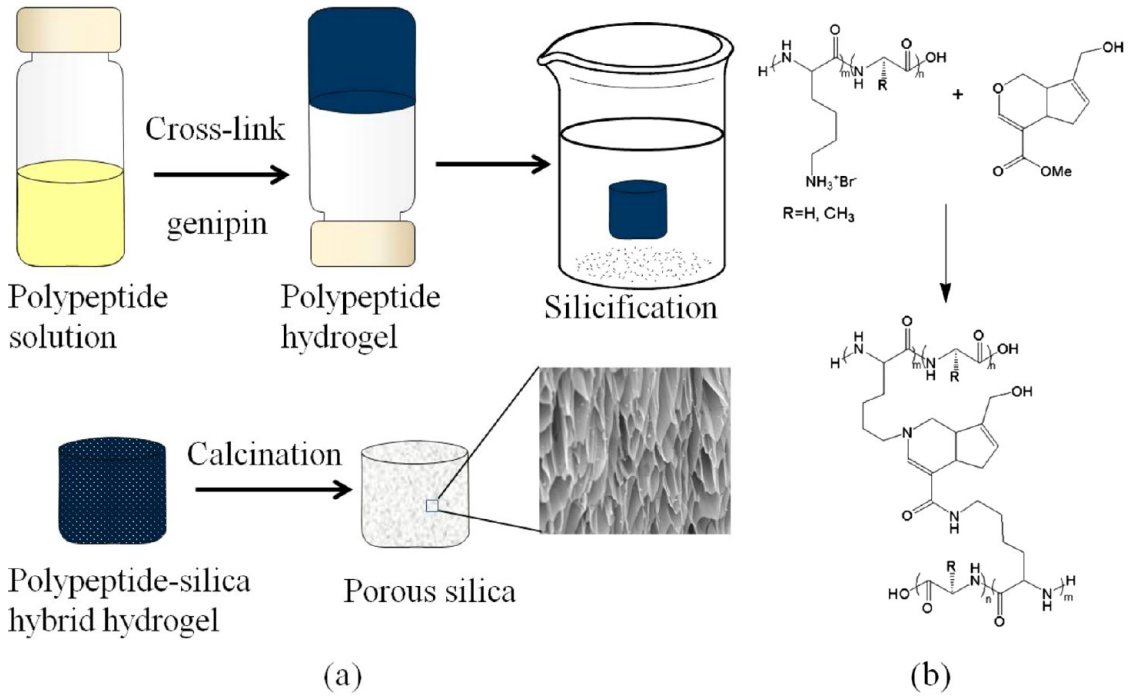

dx.doi.org/10.1021/am302016c | ACS Appl. Mater. Interfaces 2012, 4, 6865–6874

dark blue within a few hours of mixing genipin and polypeptide together. Then the polypeptides were cross-linked to form interconnected gel matrices. The cross-linked polypeptide hydrogels were dark blue in appearance due to the cross-linking reaction between genipin and the amine moieties in polypeptides (Figure 1). In the present study, the hydrogels

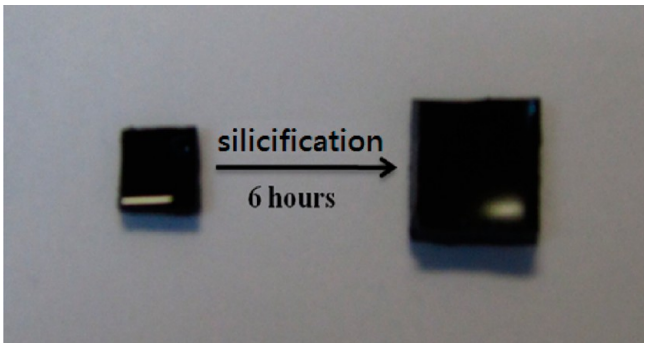

Figure 1. Photograph of cross-linked Lys_{120} hydrogel (5 wt %, left) and the as-prepared Lys_{120}–silica hybrid hydrogel (right) after 6 h of silicification.

were prepared using 5 wt % of polypeptides with genipin at 0.5 of genipin/lysine molar ratio. The as-prepared polypeptide hydrogels were subsequently immersed in 0.5 M of freshly prepared silica precursor solution for 6 h to obtain polypeptide–silica hybrid hydrogels (see Scheme 1 and Figure 1). The silicified hydrogels were then dialyzed against DI water for two days and stored in DI water for later characterization. Previously, it has been demonstrated that the polypeptide self-assemblies comprising PLL can be silicified and the precipitated silicas can translate the molecular organization.[6,8,10,14−16] Because of electrostatic interactions or hydrogen bonding between the lysine side chains and orthosilicic acid/silicate oligomers, the local concentration of silicate precursor increased in the vicinity of the lysine groups and hence polycondensation of the orthosilicic acid resulted in silica depositing onto the cross-linked polypeptide domains. In this study, it is expected that the polypeptide hydrogels with lysine residue can be hybridized by amine-induced polycondensation of orthosilicic acid. The lysine groups induced the deposition of silica onto the gel networks. It was found that silica deposition in the gel matrix was slow (on the order of hours), consistent with previous studies.[14,18,20] It can be attributed that part of the amino groups were cross-linked by genipin and, consequently, the condensation of orthosilicic acid/silicate oligomers was hindered in the cross-linked gel matrix.

The polypeptide hydrogels (5 wt %) prepared at a genipin/lysine molar ratio of 0.5 were first characterized by SEM to investigate the gel structure. The samples were prepared by freeze-drying the cross-linked hydrogels. Previously, it has been shown that the native morphology of hydrogels can be preserved by the freeze-drying procedure.[44,45] SEM analysis revealed that the freeze-dried polypeptide hydrogels exhibited interconnected membranes with macropores ranged mostly between 10 μm and 50 μm for all of these samples (for example, Figures 2a and 2b). The mechanical properties of these polypeptide hydrogels were studied by measuring their compressive strengths, which ranged between 160 and 260 kN/m^2 (see Table S1 in the Supporting Information). It can be found that the compressive strengths of these hydrogels were influenced by polypeptide chain length and composition. The mechanical strength of Lys_{120} hydrogel (227 kN/m^2) was comparable with that of Lys_{250} hydrogel. Incorporation of a short PLAla chain (DP < 30) on PLL resulted in the relatively weak hydrophobic interactions and the aggregated PLA becoming the weak region, which consequently led to the poor mechanical properties. $Lys_{330}Ala_{55}$ and $Lys_{225}Gly_{38}$ hydrogels possessed compressive strengths of 256 and 238 kN/m^2, respectively, which were higher than those of others. For the block copolypeptides with relatively long hydrophobic chains such as $Lys_{330}Ala_{55}$ and $Lys_{225}Gly_{38}$, the hydrophobic force exerted by the hydrophobic block could lead to the formation of compact structures and, subsequently, the enhancement of their mechanical properties.

The structure and composition of the as-synthesized polypeptide–silica hybrid hydrogels were then characterized by a variety of analytical techniques. SEM images showed that the silicified polypeptide hydrogels, resembling the structures of polypeptide hydrogels, exhibited interconnected networks (see Figures 2c and 2d, and Figure S2 in the Supporting Information). The results suggested that silicas specifically deposited onto the cross-linked polypeptide networks, resulting in the high-fidelity transcription of gel matrices. Comparing with the polypeptide hydrogels, the silicified hydrogels possessed much well-defined networks with rigidity, because of the deposition of silicas. It was found that the sizes of the macropores in hybrid materials (>50 μm) were much larger than those in the polypeptide hydrogels, which can be attributed to swelling during silicification process. Energy-dispersive X-ray (EDX) analysis conducted during SEM characterization showed that high contents of silicon, oxygen, and carbon elements were detected in the hybrids, indicating that the materials contained organic and inorganic compounds (see Figure S3 in the Supporting Information). FTIR analysis confirmed the deposition of silica in the polypeptide hydrogels, as evidenced by the silica absorption bands at 469 (Si–O–Si bend), 801 (Si–O–Si symmetric stretch), 960 (Si–O–H stretch), 1092 and 1207 cm^{-1} (Si–O–Si antisymmetric stretch) (see Figure 3 and Figure S4 in the Supporting Information).[15] From SEM, FTIR, and EDX analysis, the results indicated that silica precursor infiltrated into the polypeptide hydrogels and simultaneously silicas deposited along the cross-linked polypeptide membranes, resulting in the swelling of polypeptide hydrogels. It was evident that the cross-linked polypeptide matrix acted as a template for silica deposition. It can be seen that the amide I and II characteristic peaks were at 1644–1647 and 1540–1543 cm^{-1}, respectively. It suggested that the polypeptides occluded in the hybrids adopted mainly random coil conformation. The IR absorbance at 1674–1678 cm^{-1} was probably from the lysine side chain. Furthermore, the CD spectra exhibited a minimum at 199 nm and a maximum at 218 nm, which are well-known doubly inflected curve, suggesting that the polypeptides adopted mainly random coil conformation (see Figure S5 in the Supporting Information). The results from CD measurements are consistent with those from FTIR measurements. The influence of silicification time (0–8 h) on the amount of deposited silica in the hydrogels was studied using TGA measurements. Based on TGA measurements, the results revealed that the weight loss of $Lys_{150}Ala_{25}$–silica and $Lys_{120}Ala_{15}$–silica hybrid materials decreased with the increase of silicification time, indicating that the weight percentage of silica deposited in the hydrogels increased with the increase of silicification time. As the cross-linked polypeptides were

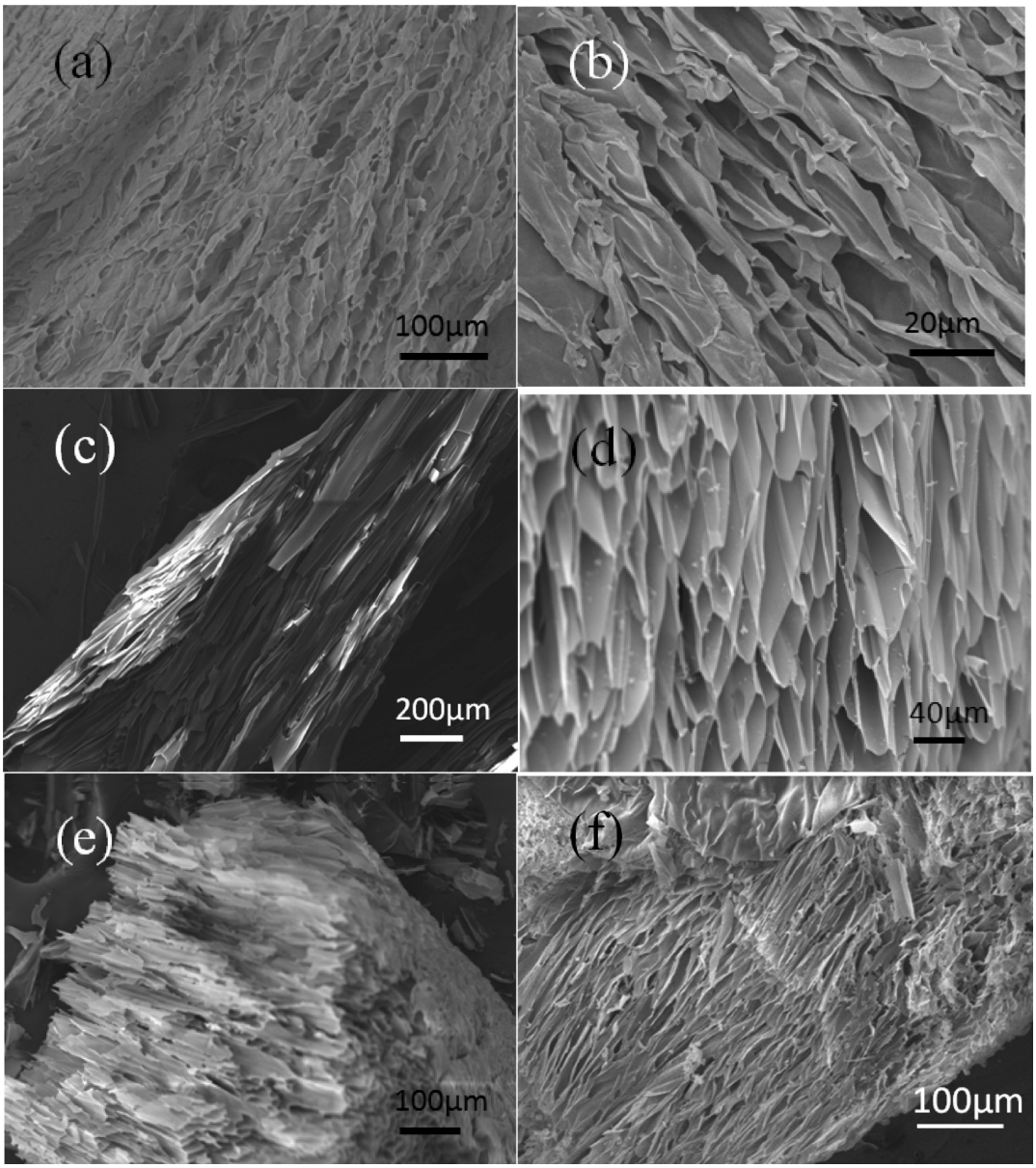

Figure 2. FE-SEM images of freeze-dried (a) $Lys_{330}Ala_{55}$ hydrogel, (b) $Lys_{150}Ala_{25}$ hydrogel, (c) $Lys_{330}Ala_{55}$–silica hybrid hydrogel, (d) $Lys_{150}Ala_{25}$–silica hybrid hydrogel, (e) silicas obtained by calcining $Lys_{330}Ala_{55}$–silica hybrid materials, and (f) silicas obtained by calcining $Lys_{150}Ala_{25}$–silica hybrid materials.

calcined to 800 °C, the weight loss was not 100%, suggesting the cross-linked polypeptides cannot be totally burned off, because of the presence of genipin (see Figure 4 and Figure S6 in the Supporting Information). EDX analysis detected the presence of silicon, oxygen, and carbon elements in the calcined materials, suggesting the as-prepared silicas containing carbon element originated from the organic compounds (see Figure S3 in the Supporting Information).

In order to gain insights on the silica nanostructures deposited on the cross-linked polypeptide matrices, the silicified hydrogels were calcined and the as-prepared silicas were studied by electron microscopy and nitrogen sorption analysis. The samples were prepared by immersing the polypeptide hydrogels in 0.5 M of freshly prepared silica precursor solution for 6 h. SEM images showed that the morphology of silicas was the replica of cross-linked polypeptide matrix (see Figures 2e and 2f, and Figure S7 in the Supporting Information). The calcined materials were not intact due to the brittleness of silicas, and the interconnected silica networks can be observed. TEM analysis revealed that the silicas were porous with sizes mostly smaller than 6 nm (see Figure 5 and Figure S8 in the Supporting Information). For comparison, hybrid materials were also characterized by TEM. TEM micrographs showed that the interconnected silica networks (dark regions) can be observed and the polypeptide nanodomains (light regions) were occluded in the silica networks (see Figure S9 in the Supporting Information). Previously, it has been demonstrated that silicas can translate the molecular organization of polypeptides such as α-helix and β-sheet.[9,14−16] Interestingly, this study suggested that genipin cross-linking led to the formation of gel matrix comprised of polypeptide nanodomains, which served as templates for silica deposition to form polypeptide–silica hybrid gel matrices. The polypeptide nanodomains adopted mainly random coil

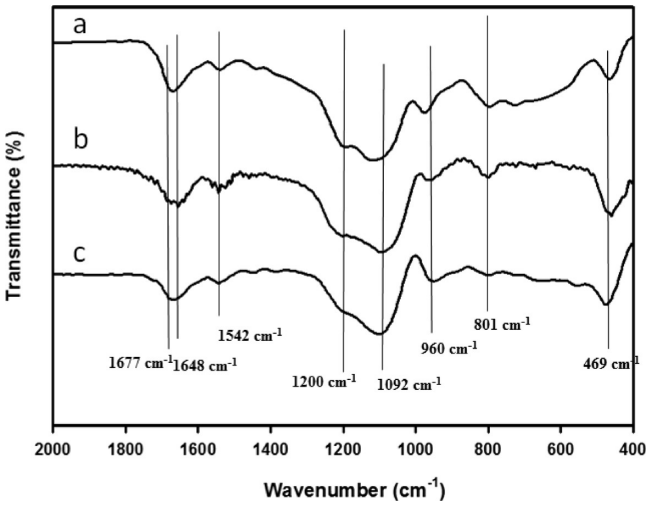

Figure 3. FTIR spectra of freeze-dried (a) $Lys_{150}Ala_{25}$–silica, (b) Lys_{120}–silica, and (c) Lys_{250}–silica hybrid hydrogels.

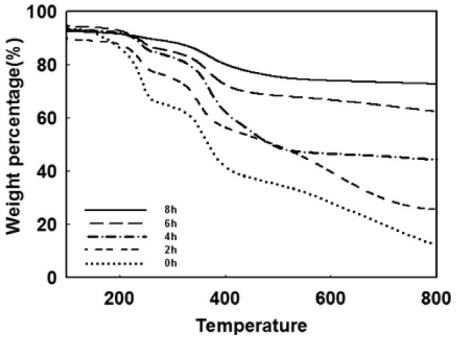

Figure 4. TGA profiles of freeze-dried $Lys_{150}Ala_{25}$ hydrogel and $Lys_{150}Ala_{25}$–silica hybrid hydrogels prepared at different silicification time.

conformation based on the results from FTIR and CD analysis. Nitrogen sorption measurements were performed to determine the influence of polypeptide chain length and composition and silicification time on the pore size and porosity. From the sorption data, the total volumes for all samples, representing the amount of nitrogen adsorbed at p/p_0 value of 0.98, ranged between 0.23 $cm^3\ g^{-1}$ and 0.46 $cm^3\ g^{-1}$ (Table 2). All of these samples possessed low micropore volume (<0.05 $cm^3\ g^{-1}$). Except the calcined Lys_{120}–silica sample, the mesopore (2–10 nm) volumes for most samples, representing the amount of nitrogen adsorbed in the pore with size between 2 and 10 nm, ranged between 0.27 and 0.37 $cm^3\ g^{-1}$. Based on BJH analysis, most of the as-synthesized silicas possessed mesopores with pore size distributions between 2 and 6 nm (Figure 6 and Figure S10 in the Supporting Information). The average pore sizes were calculated to be between 2 and 6 nm, depending on polypeptide chain length and composition (Figure 7). The additional nitrogen adsorbed beyond the mesopore volume is due to nitrogen adsorbed on the surface of the materials. The results suggested that the as-prepared polypeptide–silica hybrid network comprised of interpenetrated polypeptide nanodomains and silica. For PLL hydrogels, the polypeptide nanodomains might also form upon silicification. The introduction of silica precursor would cause the change of solution property, leading to the formation of aggregates due to the poor solvation of the cross-linked moieties and, subsequently, the deposition of silica. The calcined Lys_{120}–silica sample possessed relatively uniform pore size between 2 nm and 4 nm, compared to other samples, indicating that the polypeptide domain in the Lys_{120}–silica sample was the smallest one among all. This can be attributed that Lys_{120} chains have less entanglement and steric hindrance than the other polypeptides. In contrast, block copolypeptides would first self-assemble to form connective bilayer structures in aqueous solution and genipin cross-link would then lead to the formation of interconnected network with segregated nanodomains, which were comprised of hydrophobic segments and cross-linked moieties. It is also likely the cross-linked moieties would aggregate to form individual domains upon cross-linking. The calcined $Lys_{330}Ala_{55}$–silica sample possessed the smallest average pore size (~3.4 nm) among the calcined block copolypeptide–silica samples. This suggested that the polypeptide domain in $Lys_{330}Ala_{55}$–silica sample was the smallest among block copolypeptide–silica samples. This can be attributed to the relatively high hydrophobic interaction and chain entanglement. The results showed that the polypeptide

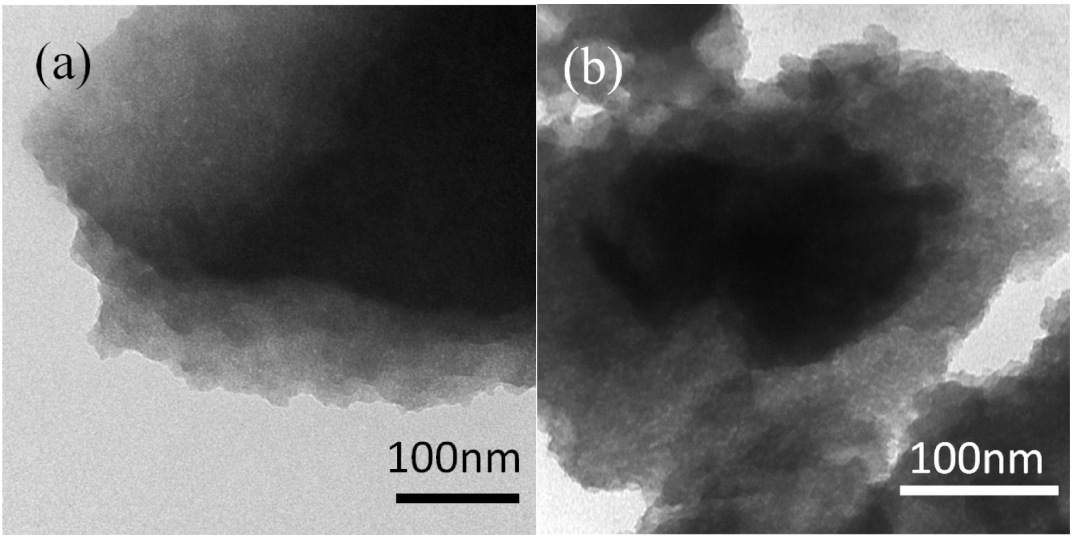

Figure 5. TEM images of silicas obtained by calcining freeze-dried (a) Lys_{330}-Ala_{55}–silica and (b) $Lys_{150}Ala_{25}$–silica hybrid hydrogels.

Table 2. Nitrogen Sorption Data of As-Prepared Silicas[a]

sample	micropore volume [$cm^3\ g^{-1}$][b]	mesopore volume (2–10 nm) [$cm^3\ g^{-1}$]	BJH pore volume [$cm^3\ g^{-1}$][c]	total pore volume [$cm^2\ g^{-1}$]	BET surface area [$m^2\ g^{-1}$]
Lys_{120}	0.040	0.116	0.136	0.236	407
Lys_{250}	0	0.336	0.351	0.386	570
$Lys_{120}\ Ala_{15}$	0	0.295	0.321	0.359	529
$Lys_{225}\ Ala_{28}$	0.001	0.317	0.334	0.376	560
$Lys_{150}\ Ala_{25}$	0.013	0.368	0.386	0.413	599
$Lys_{330}\ Ala_{55}$	0.007	0.272	0.287	0.373	624
$Lys_{225}\ Gly_{38}$	0	0.38	0.389	0.453	728

[a]The silicification time is 6 h. [b]The micropore volume was calculated using the *t*-plot method. [c]The "BJH pore volume" is the total volume adsorbed over the relative pressure range of $0.1 \le p/p_0 \le 0.9$ estimated by the BJH formalism.

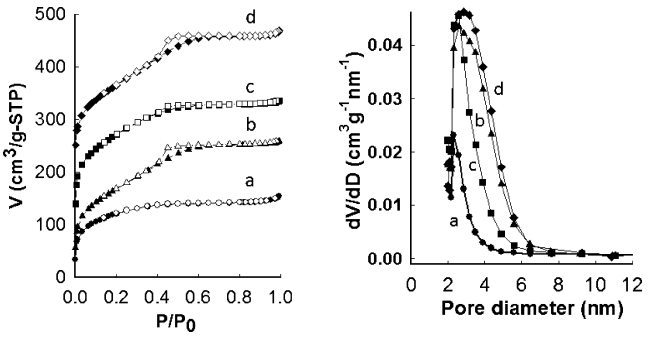

Figure 6. Nitrogen sorption isotherms (left) and pore size distributions (right) of silicas obtained from calcining (a) Lys_{120}–silica (●), (b) Lys_{250}–silica (▲), (c) $Lys_{330}Ala_{55}$–silica, (■) and (d) $Lys_{150}Ala_{25}$–silica (◆) hybrid materials. The offsets of the BET isotherms a–d are 0, 10, 95, and 200 g/cm^3-STP, respectively. The silicification time is 6 h.

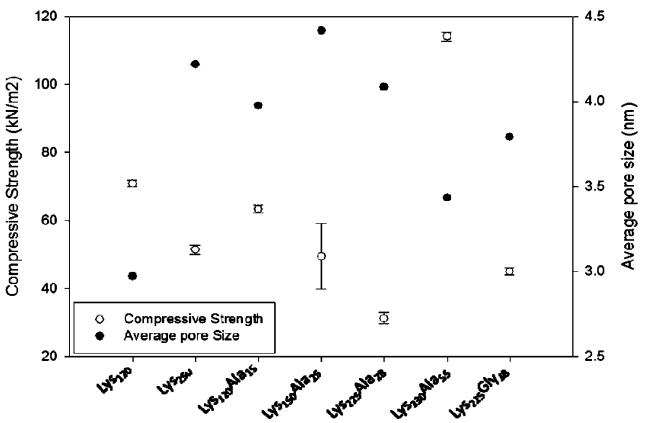

Figure 7. Compressive strength of polypeptide-silica hybrid hydrogels and average pore size possessed by silicas obtained by calcining polypeptide–silica hybrid materials.

domains were influenced by polypeptide chain length and composition, which consequently resulted in the templated silicas with different pore sizes and porosities. In addition, the silicas were also prepared by 4 h of silicification (see Table S2 and Figure S11 in the Supporting Information). The as-prepared silicas possessed higher mesopore volume and broader size distribution, compared to those obtained from 6 h of silicification, showing that the porosity of the oxides can be tuned by silicification time. One may argue that the mesoporosity of as-calcined silicas resulted from the interstitial space created by the deposition of silica. If this is the case, these hybrid materials should possess mesoporosity with sizes comparable with those of as-calcined silicas. To verify the validity of this argument, nitrogen sorption measurements were performed on the selected polypeptide–silica hybrid materials to determine their pore size and porosity. From the BJH analysis, all of the as-synthesized polypeptide-silica hybrid materials possessed mesopores with broad pore size distributions between 2 and 50 nm (see Table S3 and Figure S12 in the Supporting Information). The mesopore (2–6 nm) volumes were much lower than those of the corresponding calcined materials, suggesting that the mesoporosities of calcined materials mainly resulted from the polypeptide nanodomains.

Based on electron microscopy and nitrogen sorption analysis, silicas deposited onto the polypeptide domains on a nanoscale to form continuous network. The hybrid hydrogels were found to have very low polypeptide/silica weight percentage (<2 wt %) and good mechanical toughness (Table 3). As demonstrated using compression testing, the silicified hydrogels can have tailorable mechanical property by varying polypeptide chain length and composition and silicification time. From the data, the strength for these samples ranged between 30 and 120 kN/m^2. It can be found that the strength of these hybrid hydrogels was influenced by polypeptide chain length and the length of the hydrophobic segment. Lys_{120}–silica and $Lys_{120}Ala_{15}$–silica hybrid hydrogels had better compressive strength than Lys_{250}–silica and $Lys_{225}Ala_{28}$–silica hybrid hydrogels, respectively. Incorporation of PLA on the corresponding homopolypeptides with 8:1 Lys/Ala block ratio did not lead to the enhancement of the mechanical property. In contrast, for the block copolypeptides with 6:1 Lys/Ala block ratio, $Lys_{150}Ala_{25}$–silica hybrid hydrogel had poorer compressive strength than $Lys_{330}Ala_{55}$–silica hybrid hydrogel. The results revealed that the incorporation of short PLAla chain (<30 mers) on PLL may weaken the hybrid gels due to the relatively weak hydrophobic interactions. $Lys_{330}Ala_{55}$–silica hybrid hydrogel had the best compressive strength among all, even though the weight percentage of solid content is the lowest. It can be partly attributed to the relatively strong hydrophobic interaction exerted by the long PLAla chains. $Lys_{225}Gly_{38}$–silica hybrid hydrogel had poorer compressive strength than Lys_{250}–silica hybrid hydrogels, suggesting that the incorporation of coiled PGly did not enhance its property. For homopolypeptides or the block copolypeptides with comparable block ratio, it is interesting to observe that the hybrid hydrogel with better compressive strength possessed smaller polypeptide nanodomains (Figure 7). For example, $Lys_{330}Ala_{55}$–silica (or Lys_{120}–silica) hybrid hydrogel exhibited better mechanical properties and smaller polypeptide nanodomains than $Lys_{150}Ala_{25}$–silica (or Lys_{250}–silica) hybrid hydrogel. It is possible that the polypeptide nanodomains

dx.doi.org/10.1021/am302016c | ACS Appl. Mater. Interfaces 2012, 4, 6865–6874

Table 3. Compositions and Mechanical Properties of Polypeptide−Silica Hybrid Hydrogels (n = 4)

sample code[a]	polypeptide	silicification time (h)	weight loss (%)[b]	weight percentage of polypeptide and silica (%)[c]	strength (kN/m^2)
A1	Lys_{120}	6	35	1.3	70.9 ± 0.9
A2	Lys_{250}	6	36	1.6	51.4 ± 1.3
A3	$Lys_{120}Ala_{15}$	6	38	1.1	63.4 ± 1.7
A4	$Lys_{225}Ala_{28}$	6	39	1.3	31.3 ± 1.7
A5	$Lys_{150}Ala_{25}$	6	34	1.1	49.5 ± 9.7
A6	$Lys_{330}Ala_{55}$	6	35	1.1	114.1 ± 1.3
A7	$Lys_{225}Gly_{38}$	6	38	1.9	45.0 ± 1.1
B1	Lys_{250}	3	54	1.8	65.1 ± 1.0
B2	$Lys_{225}Ala_{28}$	3	55	1.8	48.4 ± 1.0
C1	Lys_{250}			2.8	90.2 ± 9.4
C2	$Lys_{330}Ala_{55}$			2.1	66.3 ± 5.4

[a]For samples C1 and C2, the hydrogels (5 wt %) were immersed in DI water for two days to reach equilibrium. [b]The variation is within 2%. [c]The variation is within 0.2%.

formed by $Lys_{330}Ala_{55}$ chains were compact due to relatively high hydrophobic interaction and consequently exhibited better mechanical properties than those formed by other block copolypeptides, resulting in the good mechanical properties of $Lys_{330}Ala_{55}$−silica (or Lys_{120}−silica) hybrid hydrogel. In addition, the polypeptide nanodomains and silica nanostructure interpenetrated with each other at nanometer scale can possibly have synergic effect on the mechanical properties of the hybrid hydrogels. Varying silicification time seemed to cause only the difference in organic and inorganic weight ratio and, hence, the difference in the mechanical property. For comparison, the mechanical properties of selected polypeptide hydrogels after reaching equilibrium in DI water (2−3 wt %) were also measured (sample C1 and C2). It can be observed that $Lys_{330}Ala_{55}$−silica hybrid hydrogel had better mechanical properties than $Lys_{330}Ala_{55}$ hydrogel (sample C1), even though $Lys_{330}Ala_{55}$−silica hybrid hydrogel had much lower weight percentage of solid content than $Lys_{330}Ala_{55}$ hydrogel. The results suggested that the synergy between cross-link, hydrophobic interaction, and silica deposition led to the enhancement of their mechanical properties.

Previously, Jones and co-workers reported the synthesis of gelatin−silica hybrid materials by condensation of silica with gelatin modified with a coupling agent. The compressive strengths of the as-prepared hybrid materials ranged between 19 kN/m^2 and 62 kN/m^2, depending on the organic/inorganic weight ratio.[25] Drisko and co-workers reported the synthesis of mesoporous silica pellets by infusing agarose gels with a silica precursor and condensation catalyst.[46] After calcination, mesoporous silica monoliths with high compressive strength ((3−25) × 10^3 kN/m^2), high surface areas, and large pore volumes can be produced. The mechanical properties of hybrid materials were not characterized. Unlike the previous studies, this study focused on hybridization of polypeptide hydrogels via amine-induced polycondensation of orthosilicic acid, resulting in hybrid networks comprised of interpenetrated polypeptide nanodomains and silica. The compressive strengths of the as-prepared hybrid hydrogels ranged between 30 kN/m^2 and 120 kN/m^2, depending on the polypeptide chain length and the length of the hydrophobic segment. Comparing with gelatin-silica hybrid materials, these hydrogel-based hybrid materials have relatively good mechanical toughness, even though they contain very low polypeptide/silica weight percentage (<2 wt %).

The in vitro cytotoxicity of selected polypeptide hydrogels and polypeptide−silica hybrid hydrogels was investigated. It has been reported that highly positively charged polypeptides were found to be cytotoxic to various types of mammalian cells.[47,48] In this study, it was found that Lys_{120} and $Lys_{150}Ala_{25}$ were found to be cytotoxic to fibroblast cells (data not shown), consistent with the previous studies.[47,48] It can be attributed to the electrostatic interaction between the cationic polypeptides and the anionic phospholipids in the cell membrane, leading to the cytotoxicity of polycations such as the lysine-containing copolymers. In contrast, Pochan reported that the hydrogels formed by poly(L-lysine)-block-poly(L-leucine) (PLL-b-PLLe) block copolypeptides via self-assembly were noncytotoxic.[49] In the present study, it was expected that genipin cross-linking and silica deposition can lower the charge density on PLL chains and consequently enhance the biocompatibility of the hydrogels. The fibroblast cells (3T3) were used for the cytotoxicity tests. As shown in Figure 8, the surviving cell detected for the

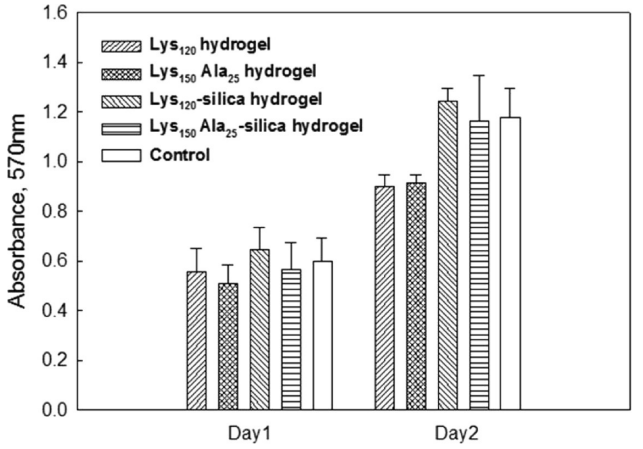

Figure 8. Cytotoxicity of Lys_{120}, $Lys_{150}Ala_{25}$, Lys_{120}−silica, and $Lys_{150}Ala_{25}$−silica hydrogels (n = 5).

cross-linked polypeptide hydrogels was higher than 80% of those for the control after 24 h. After 48 h, the cross-linked polypeptide hydrogels remained ~80% viability, compared to the control. Genipin cross-linking enhanced the biocompatibility of the hydrogels, resulting from a reduction in the charge density on PLL chains, consistent with a previous study.[49] The polypeptide−silica hybrid hydrogels showed almost 100% viability, compared with the control. The results revealed silica deposition further enhanced the biocompatibility of the hybrid hydrogels. The population of surviving cell detected between

the Lys_{120}–silica hybrid hydrogel and control showed no statically significant difference ($p > 0.01$). Also, incorporation of PLA segments in the hybrid hydrogels did not affect the number of surviving cells ($p > 0.01$). The results showed that the biocompatibility of the hydrogels can be enhanced by genipin-cross-link and silica deposition, suggesting these hydrogels were promising substrates for tissue engineering. In addition to biocompatibility, the ability for these hydrogels to promote cell attachment and proliferation is also a vital requirement for a feasible cell growth substrate. Fibroblast cells were seeded on the polypeptide hydrogels and polypeptide–silica hybrid hydrogels. After 24 h of seeding, fibroblast cells were found to grow on the polypeptide hydrogels-modified slides and were elongated spindle-shaped (Figure 9a). Also,

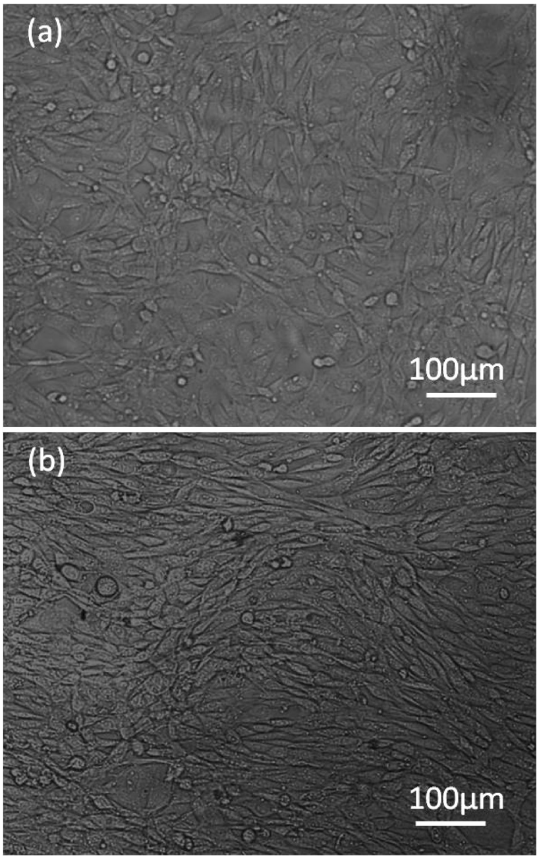

Figure 9. Optical microscopy images of fibroblast cells grown on (a) Lys_{250} hydrogel and (b) Lys_{250}–silica hybrid hydrogel after seeding for one day.

fibroblast cells grown on the polypeptide–silica hybrid hydrogels-modified slides had a spindle morphology (Figure 9b). The results indicated that the polypeptide hydrogels and polypeptide–silica hybrid hydrogels can promote cell attachment and proliferation.

CONCLUSIONS

In conclusion, we used biomimetic silicification to create well-defined silicas onto three-dimensional (3D) membranous nanostructures of cross-linked polypeptide hydrogels. By calcining the silicified hydrogels, the networks were preserved and the silicas possessed average pore sizes mostly between 2 nm and 6 nm, suggesting the formation of an interconnected network comprised of polypeptide nanodomains and silica. The compressive strength of the resulting silicified hydrogels, as well as the porosity of silicas, can be facile controlled by tuning polypeptide chain length and composition. This study highlighted that amine-catalyzed silicification can be a means to tune the constituent phases on a nanoscale and, hence, the properties of the as-prepared materials. The preliminary investigation on the cytotoxicity of the hydrogels and silicified hydrogels, as well as the cell attachment and proliferation on these hydrogels, showed that these hydrogels are potential tissue engineering scaffolds for biomedical applications. Tunable organic–inorganic composition and benign reaction conditions are also key advantages that can render this method amenable for the synthesis of green nanocomposites and biomaterials. A variety of active agents can be conjugated with PLL or encapsulated in the hydrogels, which should exert a synergic effect in biomedical use. In addition, the as-prepared mesoporous silicas might be useful as catalyst support, molecular sieving, and so forth.

ASSOCIATED CONTENT

Supporting Information

Details of all materials and measurements. This material is available free of charge via the Internet at http://pubs.acs.org.

AUTHOR INFORMATION

Corresponding Author

*E-mail: jsjan@mail.ncku.edu.tw.

Notes

The authors declare no competing financial interest.

ACKNOWLEDGMENTS

J.-S.J. acknowledges funding support from the National Science Council (Grant No. NSC100-2628-E-006-003). J.-S.J. also acknowledges T.-C. Wen for access to the glovebox, M.-C. Chen for access to the MTS machine, and K.-S. Lin for access to the nitrogen porosimetry.

REFERENCES

(1) Dickerson, M. B.; Sandhage, K. H.; Naik, R. R. *Chem. Rev.* **2008**, *108*, 4935–4978.
(2) Sanchez, C.; Arribart, H.; Guille, M. M. G. *Nat. Mater.* **2005**, *4*, 277–288.
(3) Nassif, N.; Livage, J. *Chem. Soc. Rev.* **2011**, *40*, 849–859.
(4) Chen, C.-L.; Rosi, N. L. *Angew. Chem., Int. Ed.* **2010**, *49*, 1924–1942.
(5) Meldrum, F. C.; Coelfen, H. *Chem. Rev.* **2008**, *108*, 4332–4432.
(6) Altunbas, A.; Sharma, N.; Lamm, M. S.; Yan, C.; Nagarkar, R. P.; Schneider, J. P.; Pochan, D. J. *ACS Nano* **2010**, *4*, 181–188.
(7) Holmstrom, S. C.; King, P. J. S.; Ryadnov, M. G.; Butler, M. F.; Mann, S.; Woolfson, D. N. *Langmuir* **2008**, *24*, 11778–11783.
(8) Jan, J. S.; Lee, S. J.; Carr, C. S.; Shantz, D. F. *Chem. Mater.* **2005**, *17*, 4310–4317.
(9) Kessel, S.; Thomas, A.; Boerner, H. G. *Angew. Chem., Int. Ed.* **2007**, *46*, 9023–9026.
(10) Li, Y.; Du, J.; Armes, S. P. *Macromol. Rapid Commun.* **2009**, *30*, 464–468.
(11) Meegan, J. E.; Aggeli, A.; Boden, N.; Brydson, R.; Brown, A. P.; Carrick, L.; Brough, A. R.; Hussain, A.; Ansell, R. J. *Adv. Funct. Mater.* **2004**, *14*, 31–37.
(12) Yuan, J.-J.; Zhu, P.-X.; Fukazawa, N.; Jin, R.-H. *Adv. Funct. Mater.* **2006**, *16*, 2205–2212.
(13) Hawkins, K. M.; Wang, S. S. S.; Ford, D. M.; Shantz, D. F. *J. Am. Chem. Soc.* **2004**, *126*, 9112–9119.
(14) Jan, J.-S.; Chen, P.-J.; Ho, Y.-H. *J. Colloid Interface Sci.* **2011**, *358*, 409–415.

(15) Jan, J.-S.; Chuang, T.-H.; Chen, P.-J.; Teng, H. *Langmuir* **2011**, *27*, 2834−2843.
(16) Jan, J.-S.; Shantz, D. F. *Adv. Mater.* **2007**, *19*, 2951.
(17) Ford, J.; Yang, S. *Chem. Mater.* **2007**, *19*, 5570−5575.
(18) Khripin, C. Y.; Pristinski, D.; Dunphy, D. R.; Brinker, C. J.; Kaehr, B. *ACS Nano* **2011**, *5*, 1401−1409.
(19) Wu, J.-C.; Wang, Y.; Chen, C.-C.; Chang, Y.-C. *Chem. Mater.* **2008**, *20*, 6148−6156.
(20) Xu, M. J.; Gratson, G. M.; Duoss, E. B.; Shepherd, R. F.; Lewis, J. A. *Soft Matter* **2006**, *2*, 205−209.
(21) Ruiz-Hitzky, E.; Darder, M.; Aranda, P.; Ariga, K. *Adv. Mater.* **2010**, *22*, 323−336.
(22) Vallet-Regi, M.; Colilla, M.; Gonzalez, B. *Chem. Soc. Rev.* **2011**, *40*, 596−607.
(23) Valliant, E. M.; Jones, J. R. *Soft Matter* **2011**, *7*, 5083−5095.
(24) Mammeri, F.; Le Bourhis, E.; Rozes, L.; Sanchez, C. *J. Mater. Chem.* **2005**, *15*, 3787−3811.
(25) Mahony, O.; Tsigkou, O.; Ionescu, C.; Minelli, C.; Ling, L.; Hanly, R.; Smith, M. E.; Stevens, M. M.; Jones, J. R. *Adv. Funct. Mater.* **2010**, *20*, 3835−3845.
(26) Poologasundarampillai, G.; Ionescu, C.; Tsigkou, O.; Murugesan, M.; Hill, R. G.; Stevens, M. M.; Hanna, J. V.; Smith, M. E.; Jones, J. R. *J. Mater. Chem.* **2010**, *20*, 8952−8961.
(27) Takafuji, M.; Yamada, S.-y.; Ihara, H. *Chem. Commun.* **2011**, *47*, 1024−1026.
(28) Johnson, J. R., III; Spikowski, J.; Schiraldi, D. A. *ACS Appl. Mater. Interfaces* **2009**, *1*, 1305−1309.
(29) Yuan, J. J.; Jin, R. H. *Langmuir* **2005**, *21*, 3136−3145.
(30) Deming, T. J. *Nature* **1997**, *390*, 386−389.
(31) Deming, T. J.; Curtin, S. A. *J. Am. Chem. Soc.* **2000**, *122*, 5710−5717.
(32) Gaspard, J.; Silas, J. A.; Shantz, D. F.; Jan, J.-S. *Supramol. Chem.* **2010**, *22*, 178−185.
(33) Daly, W. H.; Poche, D. *Tetrahedron Lett.* **1988**, *29*, 5859−5862.
(34) Mosmann, T. *J. Immunol. Methods* **1983**, *65*, 55−63.
(35) Slater, T. F.; Sawyer, B.; Strauli, U. *Biochim. Biophys. Acta* **1963**, *77*, 383−&.
(36) Chen, S. C.; Wu, Y. C.; Mi, F. L.; Lin, Y. H.; Yu, L. C.; Sung, H. W. *J. Controlled Release* **2004**, *96*, 285−300.
(37) Kaminski, K.; Zazakowny, K.; Szczubialka, K.; Nowakowska, M. *Biomacromolecules* **2008**, *9*, 3127−3132.
(38) Liu, T.-Y.; Lin, Y.-L. *Acta Biomater.* **2010**, *6*, 1423−1429.
(39) Mi, F. L.; Shyu, S. S.; Peng, C. K. *J. Polym. Sci. Part A: Polym. Chem.* **2005**, *43*, 1985−2000.
(40) Huang, Y.-C.; Arham, M.; Jan, J.-S. *Soft Matter* **2011**, *7*, 3975−3983.
(41) Breedveld, V.; Nowak, A. P.; Sato, J.; Deming, T. J.; Pine, D. J. *Macromolecules* **2004**, *37*, 3943−3953.
(42) Deming, T. J. *Soft Matter* **2005**, *1*, 28−35.
(43) Nowak, A. P.; Breedveld, V.; Pakstis, L.; Ozbas, B.; Pine, D. J.; Pochan, D.; Deming, T. J. *Nature* **2002**, *417*, 424−428.
(44) Hiemstra, C.; Zhou, W.; Zhong, Z.; Wouters, M.; Feijen, J. *J. Am. Chem. Soc.* **2007**, *129*, 9918−9926.
(45) Khan, F.; Tare, R. S.; Oreffo, R. O. C.; Bradley, M. *Angew. Chem., Int. Ed.* **2009**, *48*, 978−982.
(46) Drisko, G. L.; Wang, X.; Caruso, R. A. *Langmuir* **2011**, *27*, 2124−2127.
(47) Choksakulnimitr, S.; Masuda, S.; Tokuda, H.; Takakura, Y.; Hashida, M. *J. Controlled Release* **1995**, *34*, 233−241.
(48) Morgan, D. M. L.; Larvin, V. L.; Pearson, J. D. *J. Cell Sci.* **1989**, *94*, 553−559.
(49) Pakstis, L. M.; Ozbas, B.; Hales, K. D.; Nowak, A. P.; Deming, T. J.; Pochan, D. *Biomacromolecules* **2004**, *5*, 312−318.